Unburned tobacco cigarette smoke alters rat ultrastructural lung airways and DNA

Unburned tobacco cigarette smoke alters rat ultrastructural lung airways and DNA

Fabio Vivarelli, PhD[1*], Donatella Canistro, PhD[1*], Silvia Cirillo, PhD[1*], Ryan J. Elias, PhD[2], Silvia Granata, MSc[1], Matilde Mussoni, MSc[1], Sabrina Burattini, MSc[3], Elisabetta Falcieri, MD[3], Eleonora Turrini, PhD[4], Carmela Fimognari, PhD[4], Annamaria Buschini, MSc[5], Mirca Lazzaretti, PhD[5], Sofia Beghi, MSc[5], Stefano Girotti, PhD[1], Stefano Sangiorgi, MSc[1], Luca Bolelli, MSc[1], Severino Ghini, MSc[1], Elida Nora Ferri, MSc[1], Ivan Fagiolino, MSc[6], Paola Franchi, PhD[7], Marco Lucarini, MSc[7], Dario Mercatante, MSc[8], Maria Teresa Rodriguez-Estrada, PhD[8,9], Antonello Lorenzini, PhD[10], Silvia Marchionni, MSc[10], Morena Gabriele, PhD[11], Vincenzo Longo, MSc[11], Moreno Paolini, PhD[1]

[1]Department of Pharmacy and Biotechnology, Alma Mater Studiorum-University of Bologna, Via Irnerio 48, 40126, Bologna, Italy.

[2]Department of Food Science, College of Agricultural Sciences, The Pennsylvania State University, University Park, PA, 16802, USA.

[3]Department of Biomolecular Sciences, University of Urbino Carlo Bo, Campus Scientifico "E. Mattei", Via Ca' Le Suore 2, 61029, Urbino, Italy.

[4]Department for Life Quality Studies, Alma Mater Studiorum-University of Bologna, C.so d'Augusto 237, 47921, Rimini, Italy.

[5]Department of Chemistry, Life Sciences and Environmental Sustainability, University of Parma, Parco Area delle Scienze 11A, 43124, Parma, Italy.

[6]Gruppo CSA - S.p.a. Via al Torrente 22, 47923, Rimini, Italy.

[7]Department of Chemistry "G. Ciamician", Alma Mater Studiorum-University of Bologna, Via S. Giacomo 11, 40126, Bologna, Italy.

[8]Department of Agricultural and Food Sciences, Alma Mater Studiorum-University di Bologna, Viale Fanin 40, 40127, Bologna, Italy.

[9]Inter-Departmental Centre for Agri-Food Industrial Research, Alma Mater Studiorum-University of Bologna, Via Quinto Bucci 336, 47521, Cesena, Italy.

[10]Department of Biomedical and Neuromotor Sciences, Alma Mater Studiorum-University of Bologna, Via Irnerio 48, 40126, Bologna, Italy.

[11]Department of Agricultural Biology and Biotechnology, CNR, Via Moruzzi 1, 56124, Pisa, Italy.

* Equal contributed to this work

Corresponding Author: Donatella Canistro Ph.D. Department of Pharmacy and Biotechnology, Alma Mater Studiorum-University of Bologna, Via Irnerio 48, 40126, Bologna, Italy. E-mail: donatella.canistro@unibo.it

KEYWORDS: IQOS, lung damage, DNA damage, heated tobacco products, MAPK, antioxidants, oxidative stress.

Abstract: :

Introduction

Recently, the Food and Drug Administration (FDA) authorized the marketing of IQOS Tobacco Heating System as a Modified Risk Tobacco Product (MRTP) based on an electronic heat-not-burn technology that purports to reduce the risk.

Methods

Sprague-Dawley rats were exposed in a whole-body mode to IQOS aerosol for 4 weeks. We performed the chemical characterization of IQOS mainstream and we studied the ultrastructural changes in trachea and lung parenchyma of rats exposed to IQOS stick mainstream and tissue pro-inflammatory markers. We investigated the reactive oxygen species (ROS) amount along with the markers of tissue and DNA oxidative damage. Moreover, we tested the putative genotoxicity of IQOS mainstream through Ames and alkaline Comet mutagenicity assays.

Results

Here, we identified irritating and carcinogenic compounds including aldehydes and polycyclic aromatic hydrocarbons in the IQOS mainstream as sign of incomplete combustion and degradation of tobacco, that lead to severe remodelling of smaller and largest rat airways. We demonstrated that IQOS mainstream induces lung enzymes that activate carcinogens, increases tissue reactive radical concentration; promotes oxidative DNA breaks and gene level DNA damage; and stimulates mitogen activated protein kinase (MAPK) pathway which is involved in the conventional tobacco smoke-induced cancer progression.

Conclusions

Collectively, our findings reveal that IQOS causes grave lung damage and promotes factors that increase cancer risk.

Implications

IQOS has been proposed as a safer alternative to conventional cigarettes, due to depressed concentration of various harmful constituents typical of traditional tobacco smoke. However, its lower health risks to consumers have yet to be determined. Our findings

confirm that IQOS mainstream contains pyrolysis and thermogenic degradation by-products, the same harmful constituents of traditional cigarette smoke, and, for the first time, we show that it causes grave lung damage and promotes factors that increase cancer risk in the animal model.

Introduction

Purported to be a safer alternative to conventional cigarettes, "Heated Tobacco Products" (HTPs), the latest devices of the "electronic cigarette family" to which IQOS belongs, reached high popularity in recent years, especially among young people.[1] IQOS is equipped with technology that heats tobacco without combustion with a distinct appearance of cleanliness, exclusivity and high tech.[2]. Recent evidence suggest how IQOS mainstream contains various harmful constituents typical of traditional tobacco smoke such as toxic aldehydes as well as carcinogenic polycyclic aromatic hydrocarbons (PAHs) such as benzo[a]pyrene, although the concentrations are markedly lower.[3] To date, however, there are no clear evidence of a lower heath risk to consumers,[4] without considering that the World Health Organization (WHO) remarked that there is no safe level of exposure for cancer-causing chemicals.[5, 6] Meanwhile, IQOS is not banned indoors in many countries posing a serious toxicological issue since fragile groups such as pregnant women and children could be involuntary exposed. Recently, few independent studies show some toxicological outcomes similar to those elicited by traditional cigarettes.[7-10] The present study was conceived to contribute to fill the gap of knowledge on IQOS associated toxicological outcomes exploring its effects on lung's structure along with its genotoxic mutagenic and co-carcinogenic potential.

Materials and Methods

Chemical analysis on IQOS mainstream aerosol

Chemical analysis on IQOS mainstream aerosol was performed by using a customized, purpose-built smoke machine that allows for the analysis under standard conditions: puff of 2 s and 35 mL of volume and 30 s interval between two successive puffs.

The device used to perform the chemical analysis on IQOS mainstream was self-assembled including the negative pressure pneumatic system, as shown in Fig. S1A. A manually operated, three-way valve controlled the different strokes of the cycle. The reproducibility of the aspiration speed was maintained (± 2%) by fine regulation of the pressure obtained by means of labyrinths at variable pressure drop. The components connecting the smoke at the exit from IQOS to the uptake devices were designed to be as short as possible in order to reduce analyte loss. All components of this device were commercially available, except the three-way valve which was designed and built in our laboratory. The compounds analyzed in this study and the methods used are reported in Fig. S1A.

Preliminary conditions and chamber assessment

To ensure appropriate O_2/CO_2 and O_2/N_2 ratios, we set the exposure parameters in terms of puff profile and total number of HEETS consumed in order to reach a modest decrease in oxygen level (less than 5%) and a slightly higher relative CO_2 concentration, as previously described.[11] Air was sampled by the use of a Hamilton airtight syringe (30 mL), which was immediately transferred into a 5 mL capped vial and injected onto a GC/MS (QP-2010 Plus, Shimadzu, Japan) system equipped with a RTX-WAX column (30 m, 0.25 mm i.d., 0.25 µm

film thickness, Restek, USA), interfaced with a computerized system for data acquisition (Software GC–MS Solution V. 2.5, Shimadzu, Japan).

Animal exposure

Animal experiments were designed in accordance with EU Directive (2010/63/EU) guidelines, and the protocol was approved by the Committee on the Ethics of Animal Experiments of the University of Bologna and by the Italian Ministry of Health (Permit number 26832015). Twenty-four male Sprague Dawley rats (ENVIGO RMS S.r.l., San Pietro al Natisone, Udine, Italy), 7 weeks old, were housed under standard conditions (12 h light-dark cycle, 22°C, 60% humidity). After 2 weeks of acclimatization, animals were randomly assigned to control (*n*=14 rats) or exposed (*n*=10 rats) group. The exposure apparatus was comparable to those described in previous studies.[11-13] The treated group was exposed using a whole-body mode. The inhalation chamber consisted of a propylene chamber (38 × 26.5 × 19 cm) with a capacity of 19 L. The pump (0.18 kW; 1.4/1.6 A; 230 V; 50/60 Hz) was installed on one side of the box, while the IQOS aerosol was puffed on the other, generating the airflow into the chamber. The chamber containing 2 animals at a time was not hermetically sealed and the 3 holes (2 IQOS and pump connection points) were never occluded. The puff profile consisted in (5 s on, 15 s off, 5 s on) with an airflow of 4 L/min. The puff profile and flow rate were determined in accordance with previous studies on e-cigarette.[14-15] IQOS devices were powered off automatically when the stick was consumed. The exposure lasted for 20 min. Animals were submitted to aerosol from 8 tobacco sticks/day/chamber, never exceeding the 3 h/day of exposure. The concentration of nicotine recorded in IQOS aerosol mainstream was significantly lower than the LC_{50} for

vaporized nicotine in the rat model (2,3 mg/L).[16] Daily treatments were scheduled for 5 consecutive days/week followed by 2 rest days, for 4 weeks. The Animal Welfare Committee monitored the animal throughout the entire experimental program.

Scanning (SEM) and Transmission (TEM) Electron Microscopy

Trachea and lung fragments were fixed with 2.5% glutaraldehyde in 0.1 M sodium phosphate buffer for 1 h, post-fixed with 1% osmium tetroxide in the same buffer for 1 h and dehydrated in a series of progressive alcohol concentrations.[17] For SEM studies, samples were successively processed via critical point drying with liquid CO_2, attached to the specific stub and then gold sputter-coated.[18] For TEM analysis after fixation and dehydration, they were infiltrated and embedded in Araldite. When polymerized, the samples were ultra-thin sectioned, contrasted with heavy metals stains and observed by TEM.[19]

Leukocyte profile

Analyses were performed by the Central Laboratory of Clinical Pathology (CLINLAB) of the Department of Veterinary Medical Science (University of Bologna), according to standard methods certified by the Italian National Health Service.

Pro-inflammatory cytokines

Interleukins were assessed using the Multi-Analyte Elisa array microplate kit for rat inflammatory cytokines by Qiagen, in accordance with the manufacturer instructions.

Tissue cytokines gene expression

Isolation of total RNA from lung tissue was performed by Purelink RNA mini kit (Thermo Fisher Scientific, Waltham, MA, USA). The experimental procedure is available in supplementary materials.

Cytosolic and microsomal fraction isolation

The detailed procedure for obtaining the cytosolic and microsomal fractions was previously reported.[20]

Cyclooxygenase (COX) linked activity

Enzyme activity was determined spectrophotometrically in microsomal fraction following the oxidation of *NNN′,N′*-tetramethyl-p-phenylenediamine (TMPD; 100 μM) during the reduction of prostaglandin G_2 PGG_2 at 600 nm at 25°C.[21]

Analysis of radical species in lung tissue by electronic paramagnetic resonance (EPR)

The method was previously employed as an accurate measure of total radical species in different tissues.[11,13,22] Full details are available in supplementary materials.

DCFH-DA assay for ROS estimation in tissue homogenate

Tissue homogenate was mixed with 2',7'-dichlorofluorescein diacetate (DCFH-DA) assay as previously reported.[13,18] The procedure is described in supplementary materials.

Ferric reductive antioxidant power (FRAP) assay

The test was carried out following the procedure reported previously (*n=5* measurements per group).[23] Full details are available in supplementary materials.

Antioxidant enzymes

The antioxidant enzyme activities were performed spectrophotometrically on cytosolic fractions (*n=6* measurements per group).[24] Full details are available in supplementary materials.

Conjugative phase II enzymes

Glutathione S-transferase (GST) and Uridine diphosphate glucuronosyl transferase (UDPGT) were performed as previous reported. (*n=8* measurements per group).[20, 25] Procedures are described in supplementary materials.

TBARS assay

The concentration of malondialdehyde (MDA) in tissue homogenate was performed according to Seljeskog et al.[26] (*n=7* measurements per group). Further details are present in supplementary materials.

Lipid peroxides from tissue homogenate and red blood cell membranes

The FOX method, used for the estimation of lipid hydroperoxides in the tissue homogenate. The results are expressed as moles of H_2O_2/mg of protein (*n=8* measurements per group).[27, 28] Details about isolation of red cell membranes are reported in supplementary materials.

Protein carbonyl groups

The assay was performed in accordance with the method described by Levine and colleagues with some modifications.[29]

8-hydro-2-deoxyguanosine (8-OHdG) assay

The test was performed following the manufacturer's instructions (DNA/RNA oxidative damage ELISA Kit by Cayman Chemicals, (Ann Harbor, MI, USA). The DNA was extracted from tissue through QIAmp DNA investigator kit following the datasheet recommendations (QIAmp DNA investigator KIT by QIAGEN (Venlo, Netherlands) and the nucleosides were

obtained using the DNA Degradase Pus by Zymo Research Irvine, CA, USA)(*n=8* measurements per group).

Cytochrome P450 (CYP)-linked monooxygenases

p-nitrophenol hydroxylase (pNPH) was quantified by measuring 4-nitrocatechol formation at 546 nm (ε =10.28 mM^{-1} cm^{-1}). Pentoxyresorufin O-dealkylase (PROD, CYP2B1/2), ethoxyresorufin O-deethylase (EROD, CYP 1A1) and methoxyresorufin O-demethylase (MROD, CYP1A2) were determined by measuring resorufin formation spectrofluorimetrically, using pentoxyresorufin, ethoxyresorufin and methoxyresorufin as substrates respectively. (*n=7* measurements per group) As previously reported.[20]

CYP-1A1 gene expression

Total RNA was isolated from frozen lung tissues (about 20 mg) of control (*n=6* measurements per group) and IQOS (*n=6*) rats using the E.Z.N.A.® Total RNA Kit I (OMEGA Bio-tek, Norcross, GA, USA) according to the manufacturer's instruction. Further information are included in supplementary material.

SDS-page and immunoblotting

Lung protein extraction was performed employing the T-PER Tissue protein extraction reagent (Thermo Scientific, Waltham, MA, USA) and Halt Protease and Phosphate inhibitor cocktail (Thermo Scientific) following the manufacturer's recommendation. Proteins were

separated in one dimension on Bolt 4-12% Bis-tris Plus gels (Invitrogen Thermo Scientific) using a mini protean vertical gel electrophoresis mini tank module (Invitrogen Thermo Scientific). The detailed procedure is included in supplementary material section.

Mutagenicity test

Ames assay was carried out using Salmonella typhimurium TA100 strain, with and without microsomal activation (S9 mix) as described.[30, 31] The detailed procedure is included in supplementary material section.

Alkaline Comet assay

Alkaline Comet assay was performed on rat whole blood as previously reported.[11] The detailed procedure is included in supplementary material section.

Protein concentration

Protein concentrations were determined as previously described using bovine serum albumin as a standard.[32] The Pierce BCA protein assay by Thermo Scientific was employed to estimate the protein concentration for SDS-page immunoblotting.

Statistical analysis

Where not differentially specified, data are expressed as means ± standard deviation (S.D.) of measurements performed on rat samples for each studied group. Data from the preliminary tests to set the experimental conditions of the exposure chamber were analysed using Tukey's test. Cytokine gene expression analysis was performed by means of one-way ANOVA (Kruskal Wallis) followed by Dunn post hoc test. Data sets from leukocyte profile, enzyme activities, oxidative stress markers (such TBARS assay, lipid peroxides from tissue homogenate and red blood cell membranes, protein carbonyl groups, 8-hydro-2-deoxyguanosine (8-OHdG) assay) and immunoblotting were tested for normality by the D'Agostino and Pearson or Kolmogorov-Smirnov test and analysed using the two-tailed unpaired *t*-test or Mann-Whitney test in case of non-normality distribution. Data from FRAP assay 8-OHdG, and CO (n = 5 measurements per group), were analysed using the two-tailed unpaired *t*-test. The micronucleus test was statistically analysed using the two-tailed unpaired *t*-test. For the Comet assay and Ames test the distributions of the variables were preliminarily assessed by means of the one-sample Kolmogorov-Smirnov test, and parametric statistical tests were applied to normally distributed variables. The mean values from the repeated experiments were used in a one-way analysis of variance (ANOVA). If significant F-values ($P < 0.05$) were obtained, post hoc Student's t test (Bonferroni's version) was conducted for pairwise comparison. P values < 0.05 were considered statistically significant. * *P<0.05;* ** *P<0,01;* *** *P<0,001*

Results and discussion

We characterized IQOS mainstream using GC-MS based on representative tobacco smoke carcinogens (Fig. S1B-C-D) which revealed the presence of aldehydes and polycyclic aromatic hydrocarbons (PAHs). These compounds are indicative of thermal degradation and incomplete combustion of tobacco and raise questions as to whether IQOS tobacco products generate smoke rather than a generic aerosol.[3] The concentration of nicotine recorded in IQOS mainstream was significantly lower than the LC_{50} for vaporized nicotine in the rat model (2,3 mg/L) (Fig. S1D).[16] Although the present study is lacking of a comparison between harmful compounds concentration present in IQOS mainstream and those typically recorded in conventional cigarette smoke, it must be considered that the shape of the dose-response curve for chemical carcinogens, such as PAHs, deviates from the linear form,[33] and the World Health Organization (WHO) states that there is no safe level or threshold dose of exposure.[5]

Next, we show ultrastructural images of the trachea of rats exposed to IQOS stick smoking, which present histological features (Fig.1) similar to those caused by traditional cigarette smoking.[33] Images from scanning electron microscopy (SEM) of trachea specimens from control group, show a well-preserved epithelial organization, with the expected balance between goblet cells and ciliated cells (Fig 1). Exposed group reveals marked changes including the presence of erythrocytes (Fig. 1), and necrotic cells on epithelial surface (Fig. S1E g, h). Cilia distribution and length appear also affected by the treatment (Fig S1E g). Trachea details captured by SEM (Fig S1E i) and TEM (Fig S1E j-m**)** from IQOS group show secreting granules or secreting cell portions. A significant number of apoptotic and necrotic

cells appears along the submucosa (Fig. S1E k-m), including the presence of erythrocytes. These changes could be due to the aldehyde exposure, in particular acetaldehyde. [34-35] Beyond this, we observe visible apoptotic and necrotic cells (Fig. S1E k-m) in the tracheal submucosa. Lung parenchyma was markedly disrupted (Fig. 1), with deep disorganization and collapsing of the alveolar epithelium, absent bronchial branches (Fig. S1F e, f) and visible blood extravasations (Fig. S1F g). TEM revealed granulocytes pulmonary infiltration as an inflammation response (Fig. S1F h-l), which was corroborated by higher circulating blood neutrophils (Fig. S1G), typically observed in patients with stable chronic obstructive pulmonary disease (COPD).[36] These results indicate that the IQOS mainstream produced in this study is manifestly destructive to the lung.

We also find an increase in IL-13, IL-10, IL12, TNF-α and INF-δ expression (Fig. 2). IQOS exposure increases IL-10, IL-12, IL-13, TNF-α, INF-δ plasma levels. The gene expression of lung glycoprotein, granulocyte macrophage-colony stimulating factor (CSF2) and macrophage inflammatory protein CCL3 gene expression is markedly increased in the lung tissue of IQOS group compared to control group. Upregulation of pulmonary granulocyte macrophage-colony stimulating factor CSF2 can be associated to COPD progression through increasing the number of neutrophils,[37] as well as the up-regulation of macrophage inflammatory protein CCL3, which facilitates the recruitment of macrophages into the airways.[38] On the other hand, some markers here recorded such as eosinophils infiltration and the increment of Th2 cytokine IL-13 have been attributed to an asthma condition suggesting a convergence of signs,[39] and interestingly, tobacco smoke can drive eosinophils accumulation in distal airways.[40] Pulmonary cyclooxygenase (COX) linked activity is up-regulated in exposed group compared to control. Thus, IQOS mainstream is responsible for

robust inflammation. We also observe an upregulation of the pulmonary cyclooxygenase (COX), often seen in cigarette smokers, which is associated with inflammation and tumor progression.[41]

Next, the exposure to IQOS mainstream also resulted in supraphysiological production of reactive oxygen species (ROS) in the lung (Fig. S3A a, b), together with a reduction in plasma reducing potential (Fig. S3B). Unexpectedly, no significant increase in pulmonary enzymatic antioxidant and post-oxidative networks was observed (Fig. S3C a-h). The mild down-regulation of nuclear factor erythroid 2-related factor 2 (Nrf2), and the impairment of UDP-glucuronyl-transferase (Fig. S3C f, g) are often observed in patients with COPD.[42] These findings indicate that a redox imbalance results in oxidative stress (OS) and tissue injuries. To gain further insight into this, we analyzed typical OS markers, such as markers of lipid peroxidation (Fig. S3D a-c), oxidative damage to red blood cell membrane (Fig. 3D b), and protein carbonylation (Fig. S3D d). We also observed marked DNA oxidative damage as evidenced by oxidized derivatives of deoxyguanosine 8-oxo-2'-deoxyguanosine (8-oxo-dG) (Fig. 3, Fig. S3D e). These results suggest that OS causes damage not only at tissue level but also to genetic material.

Next, we explored whether the exposure to IQOS modulates the carcinogenic metabolizing cytochrome P450 (CYP) dependent enzymes that are key mediators of this catalytic process.[43] We found a marked induction of CYP1A1 and CYP2A1/2 (activating, polychlorinated biphenyls, aromatic amines, PAHs and alkylnitrosamines), CYP2B1/2 (activating olefins and halogenated hydrocarbons) and CYP2E1 (activating alcohol, nitrosamines, benzene, acetone, acrylamide) linked monooxygenases (Fig. S3E).

Interestingly, increases in such enzymes are a typical phenomenon associated with the exposure to tobacco smoke and e-cigarettes. These results suggest that IQOS increases an individual's vulnerability to the deleterious effects of both the pre-carcinogens present in the mainstream itself and the ubiquitous ones. As all these substances are rapidly bioactivated under CYP induction condition, excess carcinogenic metabolites can saturate enzymatic defense mechanisms causing damage to various macromolecules including DNA.[32,40,44] Additionally, the marked CYP1A1 induction we reveal (Fig. S3E a, b), promoting the activation of substances such as benzo[a]pyrene that are potent carcinogens but also highly toxic, is particularly harmful for distal airways which increase COPD susceptibility and progression.[45] Finally, due to the uncoupling of the CYP-Fe II-O_2 complex of the CYP catalytic cycle, CYP induction contributes to an overproduction of ROS that can lead to COPD progression, or worse, in the development of cancer.[32,42]

Accumulating evidence indicates that the mitotic-activated protein kinase (MAPK) cascade in the production of many inflammatory mediators is involved in pulmonary diseases such as asthma and COPD[46] and, recently, inhibitors of ERK/p38 MPAK have been proposed as promising agents against pulmonary inflammatory diseases.[47] Our model shows a significant activation of c-Jun N-terminal kinase (JNK), extracellular-signal-regulated kinase (ERK) 1/2 and p38 MAPK (Fig. S4A), which are typically triggered by a variety of stimuli such as proliferative signals, inflammatory, environmental insults and OS.[48] Recently, inhibitors of ERK/p38 MPAK pathway have been proposed as promising agents against pulmonary inflammatory diseases [49] NKs MAPK activation is associated with higher levels of IL-13 and TNF-α, and they enhance the transcriptional activity of AP-1, which in turn activates a wide range of immunomodulatory genes, all implicated in pulmonary diseases of diverse origin,

including pollutant-induced bronchitis, allergic and non-allergic asthma, exercise-induced asthma, acute respiratory distress syndrome and chronic obstructive pulmonary disease (COPD).[50] These data reinforce the hypothesis that IQOS consumption could worsen some inflammatory-related pulmonary disease. Interestingly, the MAPK pathway is also implicated in various aspects of cancer progression, including the lung epithelial-mesenchymal transition (EMT)[51, 52] that was recently observed in IQOS exposure in an *in vitro* model.[53]

Finally, to explore the mutagenic potential of IQOS mainstream constituents using the urine as the final repository of chemical metabolites. We found that the metabolite cocktail collected produced significant DNA damage in *S. typhimurium* as evidenced as an increase in bacterial revertants leading to gene mutation (Fig. 4). This observation is in contrast with the absence of mutagenicity of the total IQOS particulate matter reported by Philip Morris International (PMI; R&D).[54] We also observe that IQOS smoking exposure results in increased DNA damage in leukocytes identified as migration of the fragmented DNA determined by single-, double-strand breaks and alkali-labile sites (Fig. S4B); in other words, extrapolating data from the distributions of migrate nucleoids per single specimen we observe significant increases in high levels of DNA damage (99° percentile) in the IQOS group compared to controls. Given that, these results are in disagreement with the conclusions reported by PMI stating that IQOS smoking exposure cannot result in genetic material injury, further independent studies are clearly needed.

Conclusions

Our findings suggest that the IQOS unburned tobacco smoke system is by no means a low-risk product, and that the labelling of this modified-risk tobacco product may mislead consumers who interpret “a lower level of toxic compounds” as an indication of “harmlessness”. Given that considerable time is needed before data from long-term studies on cancer risk become available, we encourage regulators to continue to promote and fund independent studies that specifically address the potential toxicity of these unburned tobacco smoke systems.

Strengths and Limitation

The present is the first independent study aimed to investigate the putative genotoxic and mutagenic potential of IQOS exposure in an *in vivo* model. Images from electronic microscopes TEM and SEM give valuable information regarding the destructive effect of IQOS mainstream on airways. The study is lacking of a chemical comparison between concentration of harmful constituents recorded in IQOS mainstream and those typically detected in standard cigarette. Furthermore, the panel of genotoxicity tests could be extended in order to collect more information on the mechanism by which IQOS exposure can affect the DNA stability.

Funding: This work was supported by a grant from the Italian Ministry of Education, University and Research. S.C., S.G., S.S., D.M. PhD fellowship grants were awarded from the Italian Ministry of Education, University and Research. F.V. postdoctoral fellowship grant was cofounded by D.C., M.P., and the Department of Pharmacy and Biotechnology, University of Bologna. R.J.E. is supported in part by USDA National Institute of Food and Agriculture Federal Appropriations under Project PEN04522 and Accession no. 0233376.

Author contributions: F.V., D.C., S.C., M.P. R.J.E. designed the study. S.S, L.B., I.F., S.G., M.T.R.E., D.M. E.N.F. performed the chemical analysis. S.B., E.F. performed and analysed data from scanning/transmission microscopy. E.T., C.F., V.L., M.G. conducted the gene expression analysis. P.F., M.L. determined the ROS yield in biopsies by EPR technique. A.B., M.L., S.B., A.L., S.M., assessed the mutagenesis tests. S.C., F.V., S.G., M.M. performed animal treatment and all other *ex-vivo* assays. F.V., D.C., S.C., M.P. R.J.E. wrote the manuscript and all other reviewed and edited the paper.

Declaration of interests: The authors declare no competing interests. Data and materials availability: All data are available in the main text and in supplementary materials.

References

1. Berman ML, Glasser AM. The Public Health Standard in Action-Analysis of the US Food and Drug Administration's IQOS Review. *JAMA Oncol.* 2020;6: 1864-1865.

2. Hair EC, Bennett M, Sheen E, Cantrell J, Briggs J, Fenn Z, Willett JG, Vallone D. Examining perceptions about IQOS heated tobacco product: consumer studies in Japan and Switzerland. *Tob Control.* 2018; 27(Suppl 1):s70-s73.

3. Auer R, Concha-Lozano N, Jacot-Sadowski I, et al. Heat-not-burn tobacco cigarettes: smoke by any other name. *JAMA Intern.Med.* 2017;177:1050-1052.

4. Simonavicius E., McNeill A, Shahab L, et al. Heat-not-burn tobacco products: a systematic literature review. *Tob. Control.* 2019;28:582-594.

5. Katz MH. No smoke-just cancer-causing chemicals. *JAMA Intern. Med.* 2017;177:1052.

6. WHO. Heated tobacco products (HTPs) market monitoring information sheet. https://www.who.int/tobacco (last visit 24-4-21)

7. Leigh NJ, Tran PL, O'Connor RJ, et al. Cytotoxic effects of heated tobacco products (HTP) on human bronchial epithelial cells. *Tob. Control.* 2018;27:s26-s29.

8. Moazed F, Chun L, Matthay MA, et al. Assessment of industry data on pulmonary and immunosuppressive effects of IQOS. *Tob. Control.* 2018;27:s20–s25.

9. Davis B, To V, Talbot P. Comparison of cytotoxicity of IQOS aerosols to smoke from Marlboro Red and 3R4F reference cigarettes. *Toxicol. In Vitro.* 2019;61:104652.

10. Vu AT, Taylor KM, Holman MR, et al.Polycyclic aromatic hydrocarbons in the mainstream smoke of popular U.S. *Cigarettes. Chem. Res. Toxicol.* 2015;28:1616-1626.

11. Canistro D, Vivarelli F, Cirillo S, et al. E-cigarettes induce toxicological effects that can raise the cancer risk. *Sci. Rep.* 2017;7: 2028.

12. Cardenia V, Vivarelli F, Cirillo S, et al. The effect of electronic-cigarettes aerosol on rat brain lipid profile. *Biochimie*. 2018;153: 99-108.

13. Vivarelli F, Canistro D, Cirillo S, et al. Impairment of testicular function in electronic cigarette (e-cig, e-cigs) exposed rats under low-voltage and nicotine-free conditions. *Life Sci.* 2019;228: 53-65.

14. Havel CM, Benowitz NL, Jacob P, et al. An electronic cigarette vaping machine for the characterization of aerosol delivery and composition. *Nicotine Tob. Res.* 2017;19: 1224–1231.

15. Nabavizadeh P, Liu J, Havel CM, et al. Vascular endothelial function is impaired by aerosol from a single IQOS heatstick to the same extent as by cigarette smoke. *Tob Control*. 2018; 27:s13-s19.

16. Shao XM, Xu B, Liang J, et al. Nicotine delivery to rats via lung alveolar region-targeted aerosol technology produces blood pharmacokinetics resembling human smoking nicotine. *Tob. Res*. 2013;15: 1248–1258.

17. Burattini S, Battistelli M, Codenotti S, et al. Melatonin action in tumor skeletal muscle cells: an ultrastructural study. *Acta Histochem.* 2016;118: 278-285.

18. Cirillo S, Vivarelli F, Turrini E, et al. The customizable e-cigarette resistance influences toxicological outcomes: lung degeneration, inflammation and oxidative stress-induced in a rat model. *Toxicol. Sci.* 2019;172: 132-145.

19. Salucci S, Burattini S, Buontempo F, et al. Marine bisindole alkaloid: A potential apoptotic inducer in human cancer cells. *Eur. J. Histochem.* 2018;62: 2881.

20. Bonamassa B, Canistro D, Sapone A, et al. Harmful effects behind the daily supplementation of a fixed vegetarian blend in the rat model. *Food. Chem. Toxicol.* 2016;97: 367-374.

21. Kumar KA, Chandramohan Reddy T, Reddy GV, et al. High-throughput screening assays for cyclooxygenase-2 and 5-lipoxygenase, the targets for inflammatory disorders. *Indian J. Biochem. Biophys*. 2011;48: 256-261.

22. Fabbri R, Sapone A, Paolini M, et al. Effects of N-acetylcysteine on human ovarian tissue preservation undergoing cryopreservation procedure. *Histol. Histopathol.* 2015;30: 725–735.

23. Benzie IF, Strain JJ. The ferric reducing ability of plasma (FRAP) as a measure of "antioxidant power": The FRAP assay. *Anal. Biochem.* 1996;239: 70–76.

24. Vivarelli F, Canistro D, Sapone A, et al. Raphanus sativus cv. sango sprout juice decreases diet-induced obesity in sprague dawley rats and ameliorates related disorders. *PLoS One.* 2016;11: e0150913.

25. Canistro D, Vivarelli F, Cirillo S, et al. Comparison between in toto peach (Prunus persica L. Batsch) supplementation and its polyphenolic extract on rat liver xenobiotic metabolizing enzymes. *Food Chem Toxicol*. 2016; 97: 385-394.

26. Seljeskog E, Hervig T, Mansoor MA. A novel HPLC method for the measurement of thiobarbituric acid reactive substances (TBARS). A comparison with a commercially available kit. *Clin. Biochem*. 2006;39: 947–954.

27. Jiang ZY, Woollard AC, Wolff SP. Lipid hydroperoxide measurement by oxidation of Fe_2^+ in the presence of xylenol orange. Comparison with the TBA assay and an iodometric method. *Lipids.* 1991;26: 853-856.

28. Marchesi VT, Palade GE. The localization of Mg-Na-K-activated adenosine triphosphatase on red cell ghost membranes. *J. Cell. Biol*. 1967;35: 385- 404.

29. Levine RL, Garland D, Oliver CN, et al. Determination of carbonyl content in oxidatively modified proteins. *Methods Enzymol.* 1990;186: 464-478.

30. Maron DM, Ames BN. Revised methods for the Salmonella mutagenicity test. *Mutat. Res*. 1983;113: 173-215.

31. Yamasaki E, Ames BN. Concentration of mutagens from urine by absorption with the nonpolar resin XAD-2: cigarette smokers have mutagenic urine. *Proc. Natl. Acad. Sci. USA.* 1977;74: 3555-3559.

32. Lowry OH, Rosenbrough HJ, Farr AL, et al. Protein measurement with Folin phenol reagent. *J. Biol. Chem.* 1951;193: 265–275.

33. Armstrong BG, Gibbs G. Exposure-response relationship between lung cancer and polycyclic aromatic hydrocarbons (PAHs). *Occup. Environ. Med.* 2009;66: 740-746.

34. Simet SM, Sisson JH, Pavlik JA, et al. Long-term cigarette smoke exposure in a mouse model of ciliated epithelial cell function. *Am. J. Respir. Cell Mol. Biol.* 2010;43: 635-640.

35. Wyatt TA, Sisson JH, Allen-Gipson DS, et al. Co-exposure to cigarette smoke and alcohol decreases airway epithelial cell cilia beating in a protein kinase Cε-dependent manner. *Am. J. Pathol*. 2012;181: 431-440.

36. Pascoe SJ, Papi A,Midwinter D, et al. Circulating neutrophils levels are a predictor of pneumonia risk in chronic obstructive pulmonary disease. *Respir. Res.* 2019;20: 195.

37. Vlahos R, Bozinovski S. Role of alveolar macrophages in chronic obstructive pulmonary disease. *Front. Immunol*. 2014;5: 435.

38. Ravi AK, Khurana S, Lemon J, et al. Increased levels of soluble interleukin-6 receptor and CCL3 in COPD sputum. *Respir. Res.* 2014;15: 103.

39. van der Pouw Kraan TC, Küçükaycan M, Bakker AM, et al. Chronic obstructive pulmonary disease is associated with the -1055 IL-13 promoter polymorphism. *Genes Immun.* 2002;3: 436-439.

40. Kim SR, Rhee YK. Overlap between asthma and COPD: where the two diseases converge. *Allergy Asthma Immunol. Res.* 2010;2: 209-214.

41. Huang RY, Chen GG. Cigarette smoking, cyclooxygenase-2 pathway and cancer. *Biochim. Biophys Acta.* 2011;1815: 158-169.

42. Barnes PJ. Oxidative stress-based therapeutics in COPD. *Redox Biol.* 2020; 101544.

43. Hartog M, Zhang QY, Ding X. Role of mouse cytochrome P450 enzymes of the CYP2ABFGS subfamilies in the induction of lung inflammation by cigarette smoke exposure. *Toxicol. Sci.* 2019;172: 123-131.

44. Vivarelli F, Canistro D, Cirillo S, et al. Co-carcinogenic effects of Vitamin E in prostate. *Sci. Rep.* 2019;9: 11636.

45. Wang CD, Chen N, Huang L, et al. Impact of CYP1A1 Polymorphisms on susceptibility to chronic obstructive pulmonary disease: a meta-analysis. *Biomed. Res. Int.* 2015;2015: 942958.

46. Renda S, Baraldo G, Pelaia E, et al. Increased activation of p38 MAPK in COPDT. *Eur. Respir. J.* 2008;31: 62–69.

47. Li D, Hu J, Wang T, et al. Silymarin attenuates cigarette smoke extract-induced inflammation via simultaneous inhibition of autophagy and ERK/p38 MAPK pathway in human bronchial epithelial cells. *Sci. Rep*. 2016;6: 37751.

48. Khorasanizadeh M, Eskian M, Gelfand EW, et al. Mitogen-activated protein kinases as therapeutic targets for asthma. *Pharmaco. Ther.* 2017;174: 112-126.

49 Li D, Hu J, Wang T, et al. Silymarin attenuates cigarette smoke extract-induced inflammation via simultaneous inhibition of autophagy and ERK/p38 MAPK pathway in human bronchial epithelial cells. *Sci Rep*. 2016;6: 37751.

50. Khorasanizadeh M, Eskian M, Gelfand EW, Rezaei N. Mitogen-activated protein kinases as therapeutic targets for asthma. *Pharmacol Ther.* 2017;174: 112-126.

51. Xue X, Sun H, Xu R, et al. GADD45B Promotes glucose-induced renal tubular epithelial-mesenchymal transition and apoptosis via the p38 MAPK and JNK Signaling pathways. *Front. Physiol.* 2020;11: 1074.

52. Yu D, Geng H, Liu Z, et al. Cigarette smoke induced urocystic epithelial mesenchymal transition via MAPK pathways. *Oncotarget.* 2017;8: 8791-8800.

53. Sohal SS, Eapen MS, Naidu VGM, et al. IQOS exposure impairs human airway cell homeostasis: direct comparison with traditional cigarette and e-cigarette. *ERJ Open. Res*. 2018;5: 00159.

54. Schaller JP, Keller D, Poget L, et al. Evaluation of the tobacco heating system 2.2. part 2: chemical composition, genotoxicity, cytotoxicity, and physical properties of the aerosol. *Regul. Toxicol. Pharmacol.* 2016;81: S27-S47.

Fig. 1 IQOS exposure leads to a severe airway remodelling.

Representative images from scanning electron microscopy (SEM) of trachea specimens (upper left side bar = 20 µm) from control group, exposed group (upper right side; bar = 50 µm). Images of lung specimens (SEM) from the control group (lower left side; bar = 50 µm) and exposed animals (down right side; bar = 50 µm). A more detailed panel from SEM and TEM microscopy study is available in supplementary materials.

Fig. 2 IQOS triggers lung inflammatory response.

IQOS exposure increases IL-10, IL-12, IL-13, TNF-α INF-δ plasma levels. Pulmonary cyclooxygenase (COX) linked activity is up-regulated in exposed group compared to control. Bars represent the percentage variation of relative markers recorded in IQOS group compared with controls values arbitrary set at 100%. A more detailed panel from inflammatory markers is available in supplementary materials.

Fig. 3 IQOS exposure leads to oxidative DNA damage.

Exposed animals report higher levels of 8-OHdG as a DNA oxidative damage marker measured in DNA isolated from lung tissue (more than 300%).

Fig. 4 IQOS exposure raises the mutation rate assessed through the Ames short-term mutagenicity test.

IQOS exposure leads to a dose-dependent increase in the number of *S. typhimurium* revertants in TA100 Salmonella strain, with S9 mix, on urine. Further genotoxicity assays are available in supplementary materials.

Figure1

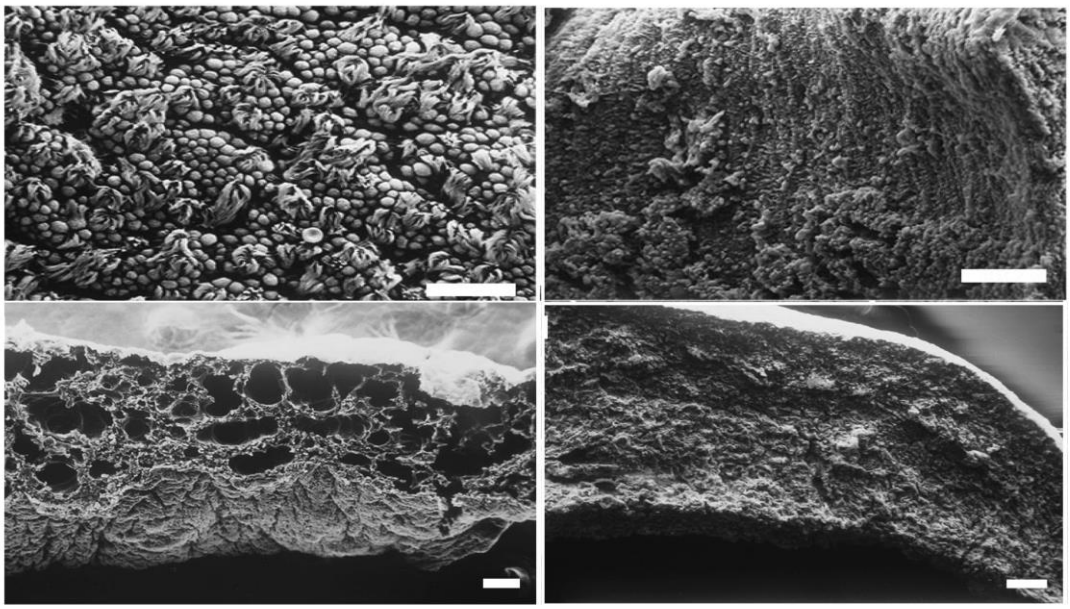

Figure_2

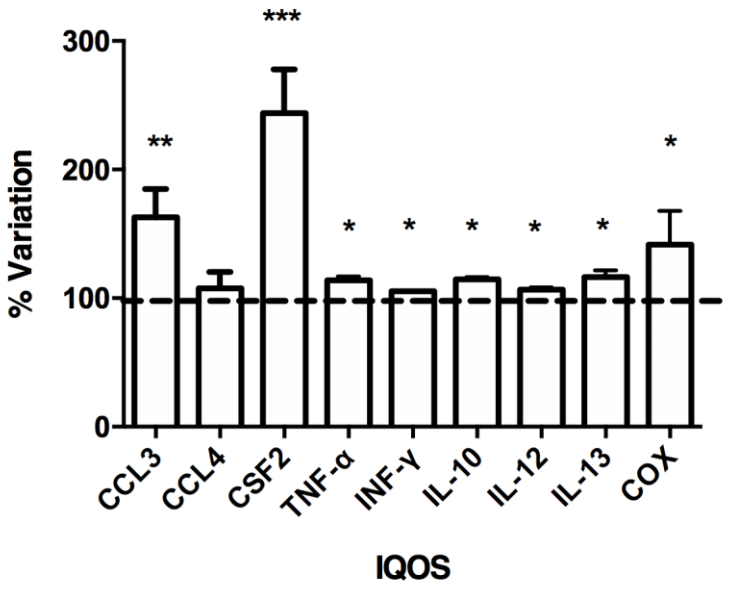

Figure_3

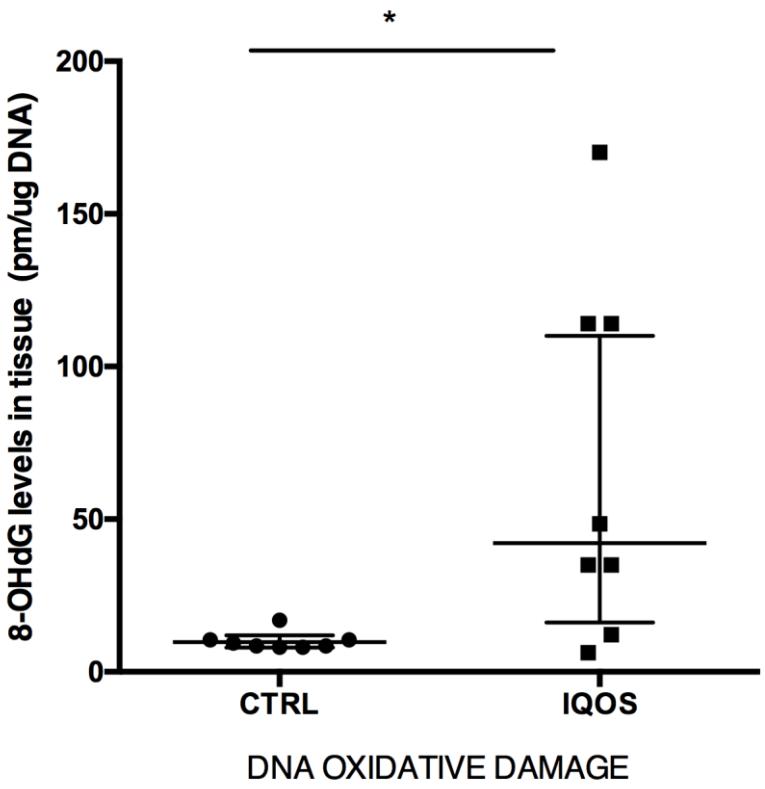
*
200
150
100
50
0
8-OHdG levels in tissue (pm/ug DNA)
CTRL
IQOS
DNA OXIDATIVE DAMAGE

Figure_4

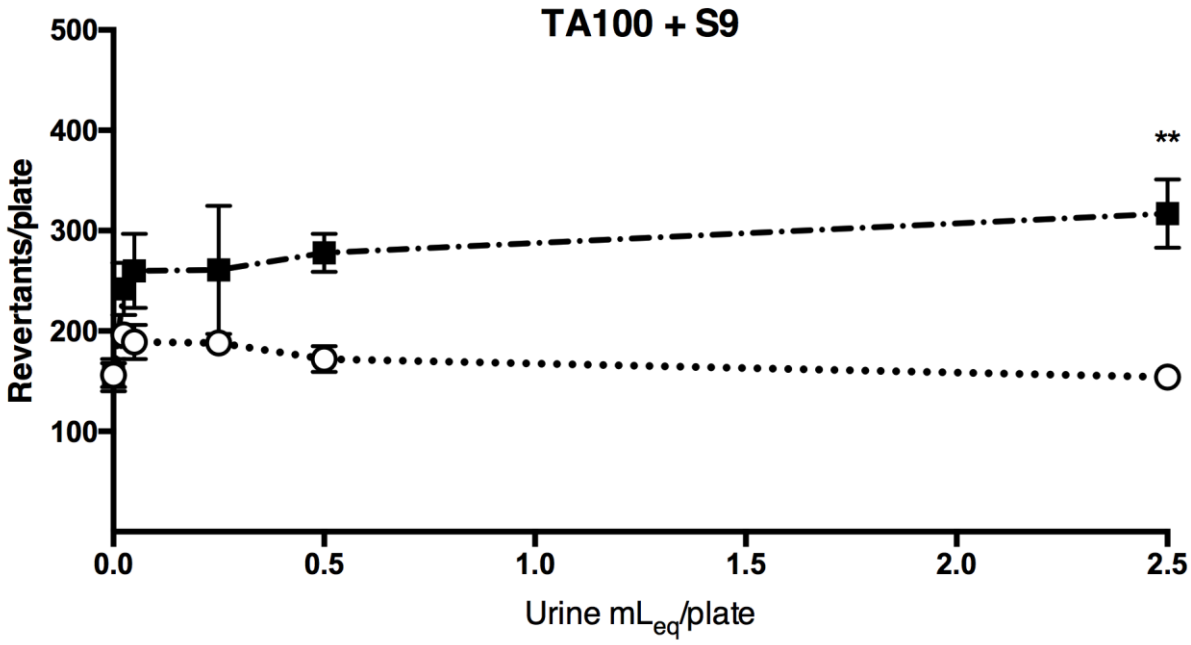
TA100 + S9
Revertants/plate
500
400
300
200
100
**
0.0
0.5
1.0
1.5
2.0
2.5
Urine mL$_{eq}$/plate